7^{th} *International Conference on* Hydroelasticity in Marine Technology
Split, Croatia, September 16^{th}-19^{th} *2015*

Rheological models of flexural-gravity waves in an ice covered ocean on large scales

Johannes E. M. Mosig[1,*], Fabien Montiel[1], and Vernon A. Squire[1]

[1] Department of Mathematics and Statistics, University of Otago, Dunedin, PO Box 56, New Zealand

Abstract. Modeling the interaction between sea ice and ocean waves is important for climate research and operational wave forecast in polar regions. To describe wave propagation in ice-covered oceans, the sea ice can be modeled by a rheological homogeneous viscoelastic layer causing waves to attenuate as they travel through the medium. Two sea ice models are considered here: (i) a viscoelastic fluid layer model and (ii) and a simpler thin viscoelastic beam model. Both models are two-dimensional. We analyze the wave modes predicted by each model and discuss the conditions under which the two models agree. We find that the complexity of the viscoelastic fluid layer model is unnecessary to predict attenuation in ice-covered seas.

Key words: *rheological models, sea ice, Euler-Bernoulli beam, viscoelasticity*

1. Introduction

Polar regions have undergone major transformations over the last three decades, with satellite and in situ observations revealing a dramatic decline of Arctic summer sea ice extent and volume [1, 2], and a moderate increase in winter Antarctic sea ice extent with significant spatial variability [3]. The magnitude and trends of such changes can only be partially captured by general circulation models, suggesting important physical processes are being neglected [4, 5, 6]. Recently it has been shown that ocean waves play an important role in controlling the morphology of polar sea ice [7, 2, 3]. As a result, much interest is currently being given to characterize the mechanisms governing the interactions between ocean waves and sea ice, and to parametrize their effects into general circulation models and operational wave models.

Near the ice edge, the ice cover is non-homogeneous and highly dynamic. It is composed of a mixture of ice floes, brash and open water, and is commonly referred to as the marginal ice zone (MIZ). The propagation of waves through the MIZ involves conservative scattering, as well as many dissipative effects

*Correspondence to: jmosig@maths.otago.ac.nz

from floe collisions, wave-breaking, turbulence, and other non-linear processes. To circumvent the difficulties of modeling such a complex physical system, a parametrization of all sources of dissipation is commonly used to model non-conservative wave attenuation. One way of doing this is to model the mixture of water and sea ice as a continuous homogeneous medium, described by a small number of rheological parameters. Wave propagation through the medium is then characterized by a dispersion relation, which provides the wavelength and attenuation coefficient of the wave modes supported by the medium. One such rheological continuum model of sea ice was recently proposed by Wang and Shen [8], who model the ice as a viscoelastic two dimensional fluid. Their model is subsequently referred to as the WS model.

In another paper which is in preparation for the Journal of Geophysical Research (herinafter MMS), we will identify some unsatisfactory aspects of the WS model when it is used to represent mixtures of ice floes and open water. A central issue is the complexity of its dispersion relation. We find that the essential features of the WS model are captured by a much simpler model, in which the ice cover is represented by a thin viscoelastic beam. The latter model is an augmented version of the dispersion relation of Fox and Squire [9], and is therefore referred to as the FS model.

As the WS model uses a fluid layer to represent the ice, wave modes can travel at the water–ice interface, the ice–atmosphere interface, or in between the two. The FS model on the other hand provides only one interface at which a flexural wave mode can travel (the elevation of the water–ice and ice–atmosphere interfaces are identical as a consequence of the thin beam mode). In the present paper, we attempt to better understand the relation between the WS and FS models by analyzing the plane wave modes the WS model predicts, recalling that both models are two-dimensional so that this is the most natural class of waves to compare. One would expect, that the two models can only agree in their predictions, if the solution of the WS model describes a pure (or possibly slightly perturbed) flexural-gravity wave mode.

The present paper is structured as follows. After introducing basic preliminaries in §2., we present the resulting dispersion relations of the two models in §3., and discuss general properties of their solutions in §4. Then, in §5. we analyze the plane wave modes corresponding to three solutions of the WS model at various shear moduli. Finally, we summarize our findings in §6.

2. Preliminaries

Consider a two-dimensional sea water domain of infinite horizontal extent, bounded above by a sea ice cover and bounded below by the sea floor. Cartesian coordinates (x, z) are defined with z pointing upwards, as depicted in figure 1. The equilibrium water–ice interface is located at $z = 0$ and the sea floor coincides with $z = -H$. The sea ice cover has uniform thickness h and is homogeneous with density $\rho = 917\,\mathrm{kg\,m^{-3}}$.

We consider the propagation of time-harmonic flexural gravity waves in the

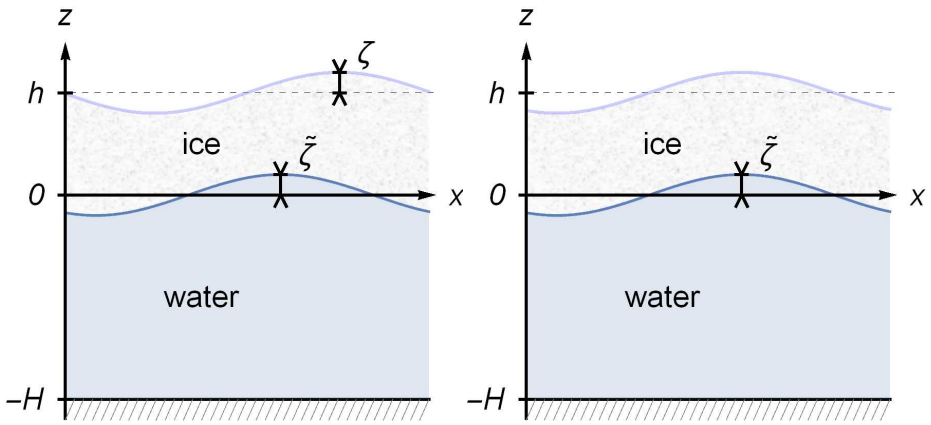

Figure 1. Sketch of the WS viscoelastic fluid model (left) and the FS viscoelastic thin beam model (right).

positive x direction, with amplitude proportional to $\exp(-\mathrm{i}\,\omega\,t)$, where ω is the angular frequency and t denotes time. The time-harmonic condition then allows us to replace $\partial_t = -\mathrm{i}\,\omega$ throughout. The sea water is assumed to be inviscid and incompressible with density $\tilde{\rho} = 1025\,\mathrm{kg\,m^{-3}}$. Therefore, its motion is fully described by a complex velocity potential $\tilde{\phi}$ satisfying the Laplace equation $\nabla^2\tilde{\phi} = 0$, as well as Bernoulli's equation

$$\mathrm{i}\,\omega\,\tilde{\rho}\,\tilde{\phi} = \tilde{\rho}\,g\,z - \tilde{P}\ , \tag{1}$$

where $\tilde{P}$ is the water pressure and $g = 9.8\,\mathrm{m\,s^{-2}}$ is acceleration due to gravity.

At the rigid sea floor the vertical velocity vanishes, i.e.

$$\partial_z\,\tilde{\phi} \;=\; 0 \quad (z = -H)\ . \tag{2}$$

At the water–ice interface, the kinematic condition is given by

$$-\mathrm{i}\,\omega\,\tilde{\zeta} \;=\; \partial_z\,\tilde{\phi} \;=\; U_z \quad (z = 0)\ , \tag{3}$$

where U_z is the z-component of the velocity field $\mathbf{U}$ of the ice layer and $\tilde{\zeta}$ is the elevation of the water–ice interface. The form of the dynamic condition depends on the ice model under consideration.

We will give a detailed derivation of the governing equations of the WS and FS models in another place (MMS). Here we just mention that both models employ a spring-dashpot model (Voigt model) for their deviatoric stress–strain relations, and thus take the same parameters as input.

3. Dispersion relations

For both models, a dispersion relation can be derived from the governing equations and boundary conditions, using plane wave ansatzes with wave number

k. After some algebra, the dispersion relation can be written in the form

$$D = \bar{D}\left(Q\,g\,k\,\tanh(H\,k) - \omega^2\right) = 0 \ , \tag{4}$$

for both ice layer models considered, where D, $\bar{D}$, and Q are functions of k and ω.

3.1. WS Model

The viscoelastic fluid layer that describes the ice in the WS model is described by a velocity potential ϕ and a stream function ψ, which can be expressed using the plane wave ansatz:

$$\phi(x,z,t) = (A\,\cosh(k\,z) + B\,\sinh(k\,z))\,e^{\mathrm{i}\,(k\,x-\omega\,t)} \tag{5}$$

$$\psi(x,z,t) = (C\,\cosh(\varphi\,z) + D\,\sinh(\varphi\,z))\,e^{\mathrm{i}\,(k\,x-\omega\,t)} \ , \tag{6}$$

where

$$\varphi^2 = k^2 - \frac{\tilde{\rho}\,\omega^2}{G_\mathrm{v}} \ . \tag{7}$$

Using this ansatz (and another plane wave ansatz for $\tilde{\phi}$), we can derive a homogeneous linear system of equations $\mathbf{M}\,\mathbf{x} = 0$ for the four unknowns $\mathbf{x} = (A,B,C,D)^T$ from the equations of motion and boundary conditions (a fifth unknown of $\tilde{\phi}$ can be eliminated by the dynamic boundary condition on the water–ice interface, see [8] for details). The dispersion relation of the WS model is therefore obtained for non-trivial solutions, i.e. $\det\mathbf{M} = 0$.

This dispersion relation can be brought into the general form given in equation (4), with $Q = Q_\mathrm{ws}$,

$$\begin{aligned} Q_\mathrm{ws} = {} & \Big(\sinh(hk)\,\sinh(h\varphi)\big(\rho^4\omega^4(N^4 - g^2k^2) + 16\varphi^2 G_\mathrm{v}^4 k^6\big) \\ & + 8\,\varphi\,G_\mathrm{v}^2\,k^3\,N^2\,\rho^2\,\omega^2\,\big(1 - \cosh(hk)\,\cosh(h\varphi)\big)\Big) \\ & / \Big(g\,k\,\rho\,\tilde{\rho}\,\omega^2\big(\rho^2\,\omega^2\,\sinh(h\varphi)(g\,k\,\sinh(hk) - N^2\,\cosh(hk)) \\ & + 4\,\varphi\,G_\mathrm{v}^2\,k^3\,\cosh(h\varphi)\,\sinh(hk)\big)\Big) + 1 \ , \end{aligned} \tag{8}$$

where

$$N = \omega - \frac{2\,k^2\,G_\mathrm{v}}{\rho\,\omega} \ . \tag{9}$$

Furthermore, $\bar{D} = \bar{D}_\mathrm{ws}$, with

$$\begin{aligned} \bar{D}_\mathrm{ws} = {} & \frac{h}{g}\Big(\big(N^2\,\cosh(h\,k) - g\,k\,\sinh(h\,k)\big)\sinh(h\,\varphi) \\ & - \frac{4\,\varphi\,G_\mathrm{v}^2}{\rho^2\,\omega^2}\,k^3\,\cosh(h\,\varphi)\,\sinh(h\,k)\Big) \ . \end{aligned} \tag{10}$$

Note that the term $\bar{D}_\mathrm{ws}$ does not appear in the original equation by Wang and Shen [8, eqn. (44)], although it was taken into account in their computations.

3.2. FS Model

For the FS model we derive $Q = Q_{\text{FS}}$, with

$$Q_{\text{FS}} \quad = \quad \frac{G_{\text{V}}\, h^3}{6\,\tilde{\rho}\, g}\,(1+\nu)\,k^4 - \frac{\rho\, h\, \omega^2}{\tilde{\rho}\, g} + 1 \ , \tag{11}$$

and $\bar{D} = \bar{D}_{\text{FS}} = 1$. We note that the dispersion relation is simpler than that of the WS model. In addition, all wave modes predicted by the FS model are flexural modes (thin beam).

4. Solutions of the dispersion relations

The two dispersion relations derived in §3. have infinitely many complex solutions. Each solution k to the dispersion relation corresponds to a plane wave mode and can be written as

$$k = \kappa + \mathrm{i}\,\alpha = \frac{2\,\pi}{\lambda} + \mathrm{i}\,\alpha \ . \tag{12}$$

where λ is the wavelength and α the attenuation rate of wave amplitude. We are only interested in forward propagating wave modes so that we only consider solutions in the first quadrant of the complex k-plane (i.e. $\lambda > 0$ and $\alpha \geq 0$). The solutions of the WS and FS models depend on five parameters: the shear modulus G, the viscosity η, the wave period $T = 2\pi/\omega$, the ice cover thickness h, and the water depth H.

For zero viscosity η, the FS dispersion relation reduces to the standard thin elastic beam dispersion relation, which has one real solution, one complex solution (with positive real and imaginary parts), and infinitely many purely imaginary solutions in the first quadrant of the complex k-plane (see e.g. [9, 10]). For non-zero viscosity, the solutions of the thin viscoelastic beam dispersion relation are slightly perturbed in the complex plane, so they all have positive real and imaginary parts. We label the perturbed real and complex solutions of the FS model k_1^{FS} and k_2^{FS}, respectively. The perturbed imaginary solutions of the FS model are not of interest here, since they describe quasi-evanescent waves with insignificant geophysical relevance. The solutions of the FS model can be seen in figure 2. (right panel) for values of the parameters (G, η, T, h, H) = (10 Pa, 1 m^2 s^{-1}, 6 s, 1 m, 100 m).

The solutions of the WS model are not as simply organized in the complex plane as those of the FS model. In particular, setting the viscosity to zero we find a large number of complex solutions (with positive real and imaginary parts) scattered over the first quadrant, in addition to a large (probably infinite) number of imaginary solutions and several real solutions. As with the FS model, all the solutions are perturbed in the first quadrant of the complex plane when a small viscosity term is introduced.

We give unique labels to the various solutions of the WS model at (G, η, T, h, H) = (10 Pa, 1 m^2 s^{-1}, 6 s, 1 m, 100 m). This set has been chosen so that the

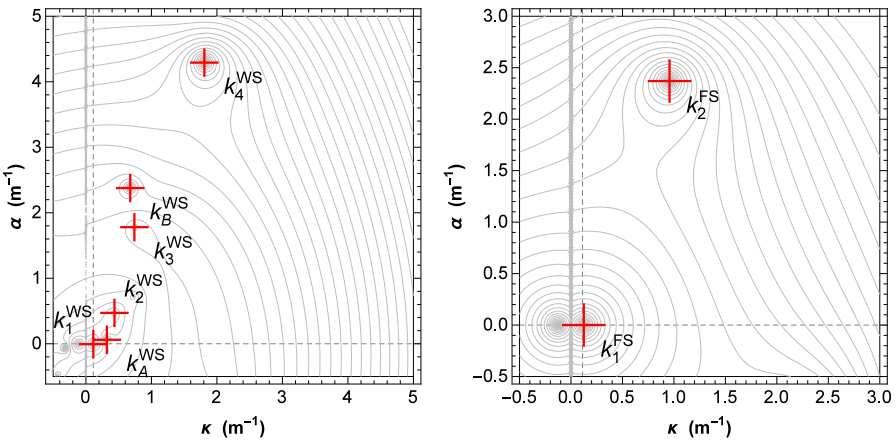

Figure 2. Selected contours of $|D_{\mathrm{WS}}(\kappa+\mathrm{i}\,\alpha)|$ (left) and $|D_{\mathrm{FS}}(\kappa+\mathrm{i}\,\alpha)|$ (right) with roots indicated by red crosses. Dashed lines indicate $\alpha = 0$ and $\lambda = \lambda_0$, where λ_0 is the open water wavelength. Note, that the rich structures of the dispersion relations along the α-axes appear as solid lines. For this plot the standard parameter set $(G,\ \eta,\ T,\ h,\ H) = (10\,\mathrm{Pa},\ 1\,\mathrm{m}^2\,\mathrm{s}^{-1},\ 6\,\mathrm{s},\ 1\,\mathrm{m},\ 100\,\mathrm{m})$ was employed.

solutions are well separated and can be identified in the contour plot shown in figure 2. (left panel). We designate the roots of $\bar{D}_{\mathrm{WS}}$ (see eq. (10)) by $k^{\mathrm{WS}}A$ and $k^{\mathrm{WS}}B$ and the other solutions by k_1^{WS}, k_2^{WS}, k_3^{WS}, k_4^{WS}, ordered by increasing distance from the origin. More solutions exist beyond the domain depicted in figure 2., and very close to the imaginary axis, but they are not physically relevant. In principle these solutions may become physically relevant as the parameters are changed, but in the following we disregard this possibility and focus on the solutions highlighted in figure 2.

Wang and Shen devised two criteria to identify the dominant solution k_{dom}^{WS} of the dispersion relation that has most geophysical relevance, i.e. carries the most wave energy. Specifically, they defined a solution to be dominant if and only if (i) the wave number is closest to the open water value, and (ii) the attenuation rate is the least among all modes. We also use these criteria, although for some parameter configurations no solution satisfies both criteria, in which case we keep criterion (i) only. In all the cases we simulated, we found that k_{dom}^{WS} was always k_1^{WS}, k_2^{WS}, or $k^{\mathrm{WS}}A$. In the FS model, the dominant solution was always k_1^{FS}.

5. Modes of the WS model

In figure 3., the solutions k_1^{WS}, k_2^{WS}, and k_3^{WS} of the WS model, as well as the solutions k_1^{FS} and k_2^{FS} of the FS model, are shown for various shear moduli

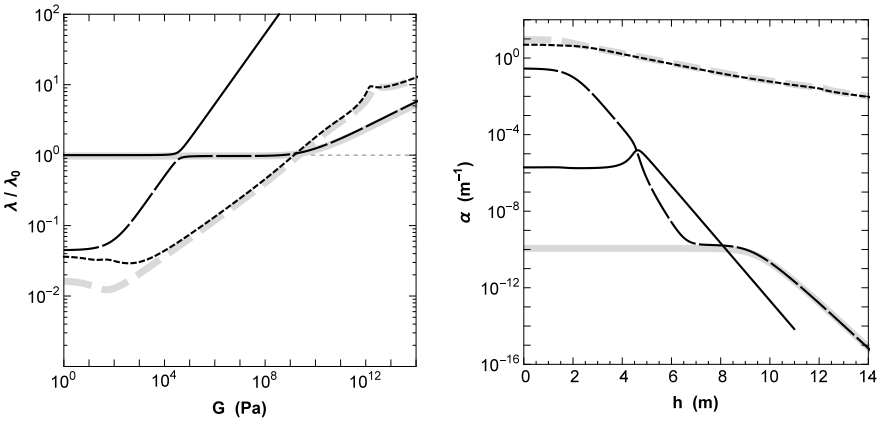

Figure 3. Relative wavelengths λ/λ_0 (left) and attenuation coefficients α (right) for various shear moduli G. The depicted solutions of the WS model are k_1^{WS} (thin, solid), k_2^{WS} (thin, long dashes), and k_3^{WS} (thin, short dashes). Thick solid gray lines represent the dominant solution k_1^{FS} of the FS model. Thick dashed gray lines represent k_2^{FS}. For these plots we chose $\eta = 0.05\,\mathrm{m}^2\,\mathrm{s}^{-1}$, $T = 8\,\mathrm{s}$, $h = 0.5\,\mathrm{m}$, and $H = 100\,\mathrm{m}$.

G. The left panel shows the wavelength $\lambda = 2\,\pi/\mathrm{Re}(k)$, scaled by the open water wavelength λ_0, and the right panel shows the wave amplitude attenuation coefficient $\alpha = \mathrm{Im}(k)$ for each solution. According to the criteria (i) and (ii), introduced in §4., k_1^{WS} is dominant for $G \leq 3.8 \times 10^4\,\mathrm{Pa}$ and k_2^{WS} is dominant for larger shear moduli. For the FS model, k_1^{FS} is always dominant. One can see, that for high G the WS and FS models agree well in their dominant solutions. We also note that there is a good agreement between k_3^{WS} and k_2^{FS} when $G \geq 10^4\,\mathrm{Pa}$. A proper comparison between the WS and FS models will be published elsewhere (MMS).

Here we want to take a closer look at the physical meaning of the solutions of the WS model. Specifically, we look for a correlation between the mode types and the correspondence to the FS model. As was mentioned before, the dispersion relation of the WS model describes waves traveling on and between the two interfaces: the water–ice and the ice–atmosphere interface. In contrast, the FS model describes flexural waves of a thin beam ice sheet only.

Up to a scale factor we can determine the constants A, B, C, and D in equations (5) and (6) by finding the eigenvector of $\mathbf{M}$ corresponding to the eigenvalue zero. Then, we can construct the velocity potential ϕ and stream function ψ describing the ice cover in the WS model. Using the time harmonic condition and the definition of the velocity field $\mathbf{U}$, we can derive the particle displacement $\mathbf{R} = \mathrm{i}\,\omega^{-1}\,\mathbf{U}$ within the ice. Its z-component R_z at $z = 0$ is the elevation $\tilde{\zeta}$ of the water–ice interface, and at $z = h$ it is the elevation ζ of the ice–atmosphere interface. One can also imagine waves propagating at intermediate

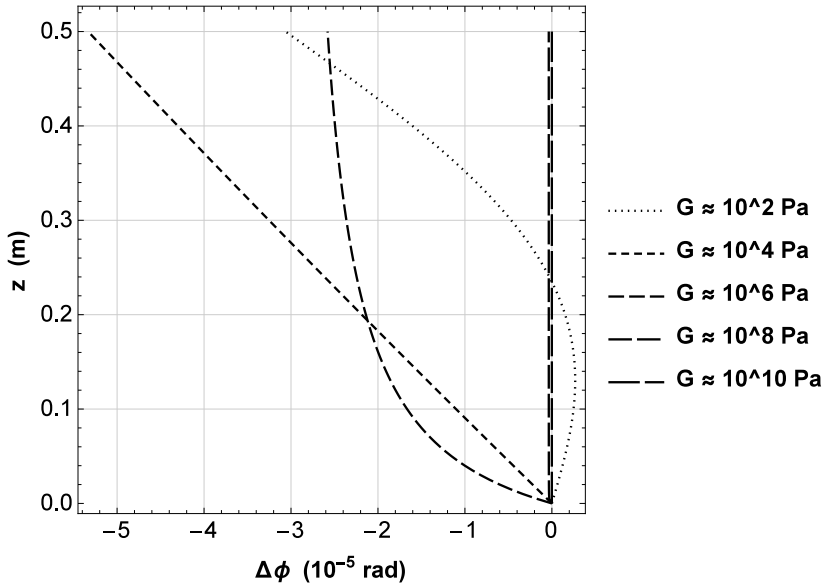

Figure 4. Phase profiles of k_1^{WS} for various G. The parameters are the same as in figure 3.

layers, where $0 < z < h$.

To depict the wave modes that correspond to a particular solution k of the dispersion relation $\det \mathbf{M} = 0$, we analyze the difference in phase $\Delta\phi(z)$ between $R_z(z)$ and $\tilde{\zeta} = R_z(0)$, i.e.

$$\Delta\phi(z) = \arg(R_z(z)) - \arg(R_z(0)) \; . \tag{13}$$

When $\Delta\phi(h) = 0$, the two interfaces are in phase, which is what we would expect from a flexural mode. When $\Delta\phi(h) = \pi$, the maxima of the water–ice interface correspond to minima of the ice–atmosphere interface, which is what we would expect for a pressure wave mode, propagating in positive x-direction. But the dispersion relation of the WS model has solutions that correspond to modes which fall into neither category, which is why we also look at the intermediate sections of the ice layer to get an idea of their nature.

Figure 4. shows the phase profile $\Delta\phi(z)$ of the solution k_1^{WS} (thin solid black lines in figure 3.) for various shear moduli G. We chose to investigate the case of non-zero viscosity $\eta = 0.05\,\mathrm{m^2\,s^{-1}}$ and thickness $h = 0.5\,\mathrm{m}$, as in figure 3. At first we observe that all sections of the ice layer are almost in phase with each other (note the scale on the $\Delta\phi$-axis), but for small shear moduli, slight variations occur. Therefore, k_1^{WS} describes slightly perturbed flexural modes for all G. At $G = 10^2\,\mathrm{Pa}$ and $10^6\,\mathrm{Pa}$, $\Delta\phi(z)$ is not a linear function as for $G = 10^4\,\mathrm{Pa}$, but curved towards negative and positive phase, respectively. For $G \geq 10^8\,\mathrm{Pa}$ the phase variation is at least two orders of magnitude smaller, and therefore k_1^{WS} is

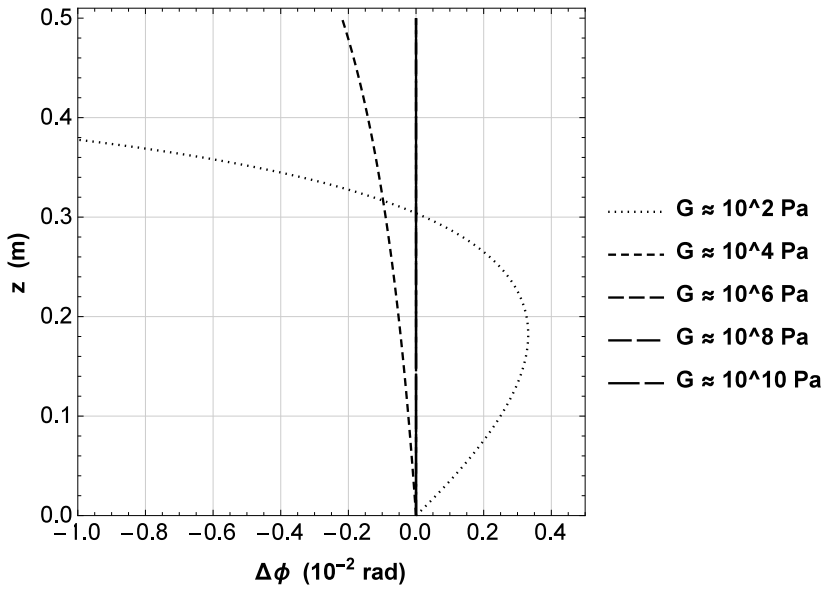

Figure 5. Phase profiles of k_2^{WS} for various G. The parameters are the same as in figure 3. Note the different scale of the $\Delta\phi$-axis.

then very close to describing a perfect flexural mode.

We now analyze the phase profile of the second solution k_2^{WS} (thin, long dashed lines in figure 3.) in figure 5. The overall appearance is similar to the phase profile of k_1^{WS}, but the scale of the phase deviations is three orders of magnitude larger. In fact, at $G = 10^2$ Pa the two interfaces are shifted in phase by almost π (this can be seen on a figure with different scale of $\Delta\phi$-axis), so k_2^{WS} describes a perturbed pressure wave mode. As G increases, the phase shift rapidly drops, and almost vanishes for $G \geq 10^6$ Pa. Note that for $G \gtrsim 10^4$ Pa, k_2^{WS} agrees with k_1^{FS} of the FS model in terms of wavelength, and for $G \gtrsim 10^6$ Pa, where k_2^{WS} describes a perturbed flexural mode, k_2^{WS} and k_1^{FS} are almost identical (see figure 3.).

Finally we have a look at the phase profile of the secondary solution k_3^{WS}, depicted in figure 6. We call it the secondary solution, because it seems to correspond to k_2^{FS}, at least for $G \geq 10^4$ Pa. The phase profile of k_3^{WS} looks qualitatively very different from the profiles of k_1^{WS} and k_2^{WS}. At $G = 10^2$ Pa, the two interfaces show a relative phase of $\Delta\phi(h) \approx 0.1$ rad, while intermediate sections show a much lager shift. For $G \geq 10^3$ Pa, the two interfaces are almost in phase, but the intermediate sections of the ice layer again show a considerable phase shift, apparently almost symmetrical about the section $z = h/2$. As G increases, the deviation declines until all sections are in phase with each other for $G \gtrsim 10^7$ Pa. Thus, k_3^{WS} transforms from a perturbed pressure wave into a perturbed flexural wave. Correspondingly, k_3^{WS} approaches k_2^{FS} as G increases, and the two solu-

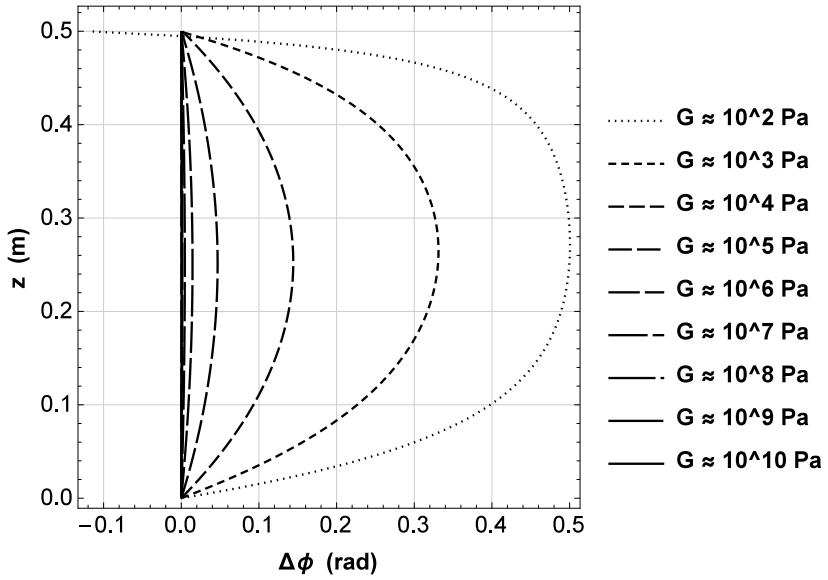

Figure 6. Phase profiles of k_3^{WS} for various G. The parameters are the same as in figure 3.

tions appear very similar in figure 3., when $G \geq 10^4\,\mathrm{Pa}$ were the interfaces are in phase.

6. Summary and conclusions

In the present paper we compared two continuum rheological models of sea ice: the WS model, representing the ice layer by a viscoelastic fluid, and the FS model, representing the ice layer by a viscoelastic thin beam. We will provide a comprehensive analysis in another paper (MMS), showing that the dominant solution of the FS model corresponds to the dominant solution of the WS model, if the shear modulus G (or viscosity η) is large enough. We also found a correspondence between two solutions which we label k_3^{WS} and k_2^{FS}. Each solution to the WS dispersion relation describes a plane wave mode traveling at and in between the water–ice and ice–atmosphere interfaces. In the present paper, we attempt to understand the correspondence between the WS and FS models by analyzing for three solutions k_1^{WS}, k_2^{WS}, and k_3^{WS} the phase difference between wave modes propagating at various sections of the ice layer, expecting that the WS and FS solutions can only coincide whenever the WS solution describes a pure flexural wave mode.

We found that for all three solutions k_1^{WS}, k_2^{WS}, and k_3^{WS}, the water–ice and ice–atmosphere interfaces, as well as all intermediate sections are in phase when the shear modulus is sufficiently high, as one would expect. Furthermore, k_1^{WS}

describes a slightly perturbed flexural mode, regardless of G, even though it does not agree with any solution in the FS model (it only matches in wavelength with k_1^{FS} for low G). Solution k_2^{WS} behaves similar to k_1^{WS}, but the perturbation is larger, and for small G it abruptly changes into a perturbed pressure wave mode, in which case it stops resembling the solution k_1^{FS} of the FS model, as expected. Finally, for k_3^{WS} the boundaries of the ice layer are in phase for $G > 10^2$ Pa, but the intermediate layers of the ice are out of phase and one may classify these modes as perturbed flexural modes, which allows it to agree with k_2^{FS} of the FS model.

We conclude that slightly perturbed flexural modes correspond to solutions of the WS model that may agree with some solution of the FS model, but it is not a sufficient condition, i.e. there are perturbed flexural modes of the WS model (such as k_1^{WS}) which do not correspond to any solutions of the FS model. Therefore, to understand the relation between the predictions of the two models, further investigations are required. Nevertheless, as we will show in another paper (MMS), the FS model has several advantages over the WS model and is able to make the same predictions when calibrated and tested with experimental data.

Acknowledgements

JM is supported by the University of Otago Postgraduate Scholarship. FM and VS are supported by the Office of Naval Research Departmental Research Initiative Sea State and Boundary Layer Physics of the Emerging Arctic Ocean (award number N00014-131-0279), the EU FP7 Grant (SPA-2013.1.1-06), and the University of Otago. The authors have enjoyed discussions with Professor Hayley Shen and Dr. Erik Rogers, which have improved the work reported in this paper.

References

[1] W. N. Meier, D. Gallaher, and G. G. Campbell. New estimates of Arctic and Antarctic sea ice extent during September 1964 from recovered Nimbus I satellite imagery. *The Cryosphere*, 7(2):699–705, 2013.

[2] R. Kwok and D. A. Rothrock. Decline in Arctic sea ice thickness from submarine and ICESat records: 1958-2008. *Geophysical Research Letters*, 36(15), 2009.

[3] Graham R. Simpkins, Laura M. Ciasto, and Matthew H. England. Observed variations in multidecadal Antarctic sea ice trends during 1979-2012. *Geophysical Research Letters*, 40(14):3643–3648, 2013.

[4] Julienne Stroeve, Marika M. Holland, Walt Meier, Ted Scambos, and Mark Serreze. Arctic sea ice decline: Faster than forecast. *Geophysical Research Letters*, 34(9), 2007.

[5] Martin O. Jeffries, James E. Overland, and Donald K. Perovich. The Arctic shifts to a new normal. *Physics Today*, 66(10):35, 2013.

[6] S. Tietsche, J. J. Day, V. Guemas, W. J. Hurlin, S. P. E. Keeley, D. Matei, R. Msadek, M. Collins, and E. Hawkins. Seasonal to interannual Arctic sea ice

predictability in current global climate models. *Geophysical Research Letters*, 41(3):1035–1043, 2014.

[7] I. R. Young, S. Zieger, and A. V. Babanin. Global Trends in Wind Speed and Wave Height. *Science*, 332(6028):451–455, 2011.

[8] Ruixue Wang and Hayley H. Shen. Gravity waves propagating into an ice-covered ocean: A viscoelastic model. *Journal of Geophysical Research*, 115(C6), 2010.

[9] Colin Fox and Vernon A. Squire. On the oblique reflexion and transmission of ocean waves at shore fast sea ice. *Philosophical Transactions of the Royal Society of London. Series A*, 347(1682):185–218, 1994.

[10] David V. Evans and Thomas V. Davies. *Wave-ice Interaction.* Castle Point Station, Davidson Laboratory, Stevens Institute of Technology, 1968.